

# Prediction of Milling Force Coefficients From Orthogonal Cutting Data

E. Budak

Y. Altıntaş

Department of Mechanical Engineering,  
The University of British Columbia,  
Vancouver, BC, Canada V6T 1Z4

E. J. A. Armarego

Department of Mechanical and  
Manufacturing Engineering,  
University of Melbourne,  
Parkville, Victoria 3052, Australia

*The mechanistic and unified mechanics of cutting approaches to the prediction of forces in milling operations are briefly described and compared. The mechanistic approach is shown to depend on milling force coefficients determined from milling tests for each cutter geometry. By contrast the unified mechanics of cutting approach relies on an experimentally determined orthogonal cutting data base (i.e., shear angle, friction coefficient and shear stress), incorporating the tool geometrical variables, and milling models based on a generic oblique cutting analysis. It is shown that the milling force coefficients for all force components and cutter geometrical designs can be predicted from an orthogonal cutting data base and the generic oblique cutting analysis for use in the predictive mechanistic milling models. This method eliminates the need for the experimental calibration of each milling cutter geometry for the mechanistic approach to force prediction and can be applied to more complex cutter designs. This method of milling force coefficient prediction has been experimentally verified when milling Ti<sub>6</sub>Al<sub>4</sub>V titanium alloy for a range of chatter, eccentricity and run-out free cutting conditions and cutter geometrical specifications.*

## 1 Introduction

Reliable quantitative predictions of the cutting force components in machining operations are essential for determining the power requirements, machined component geometrical errors or deviations, chatter vibration characteristics and strength requirements of cutting tools and jigs and fixtures in designing and selecting practical machining systems. Force predictions are also required for arriving at constrained optimization strategies in computer-aided process planning.

Traditionally the forces in practical machining operations have been established by empirical approaches whereby the effects of the more obvious process variables such as the feed, depth of cut and cutting speed have been related to the experimentally measured average force components by means of curve fitted (or empirical) equations. Examples of such equations for turning, drilling and milling can be found in the literature, some handbooks and well established textbooks in machining (Boston et al., 1937; Armarego and Brown, 1969). In practical milling operations, where the radial cut thickness and associated forces can fluctuate cyclically during a cutter revolution (Martelotti, 1941), semi-empirical or mechanistic approaches have been used to predict the force components for specified cutting conditions. In these approaches milling force component coefficients for relating the force to chip load are established from experimental milling force tests for a given cutter geometry and tool-workpiece material combination using curve fitting technique, i.e., an empirical approach. These empirically established milling force component coefficients may then be used in the mechanistic analyses or models for predicting the instantaneous force components and their fluctuations during a cutter revolution as well as the average forces and power (Koenigsberger and Sabberwal, 1961). The mechanistic approach has been applied to end milling for predicting the force fluctuations for rigid as well as flexible cutter-workpiece systems and also extended to predict the associated machine component or surface geometrical errors (Tlustý and McNeil, 1975;

Kline et al., 1982; Yellowley, 1985; Sutherland and DeVor, 1986; Montgomery and Altıntaş, 1991; Smith and Tlustý, 1991; Budak and Altıntaş, 1992a, 1992b). Some of the earlier attempts at force prediction only considered the tangential force in order to predict the power while the later attempts considered two force components in the working plane normal to the cutter axis.

Despite the increased sophistication and usefulness of the mechanistic models developed in recent years, the predictive capability of the force and surface error predictions rely on the empirically established milling force component coefficients for each cutter design. Hence in order to allow for changes in the cutter geometrical design and specification new sets of milling force component coefficients have to be experimentally established from milling tests for each design. Thus a prohibitive amount of testing may be necessary particularly when more complex milling cutter designs, such as helical ball end mills with variable geometry along to the tooth edges (Yucesan and Altıntaş, 1996) are to be catered for. Although such procedures are useful for a quick identification of cutting coefficients for an existing cutter, they may be considered costly and impractical for process planners and tool designers for the preparation of a general data base.

An alternative "fundamental" or "unified mechanics of cutting" approach for predicting all force components, torque and power in a variety of practical machining operations such as turning, drilling and milling has been established and is being extended by ongoing research (Armarego et al., 1983, 1985, 1990, 1993). This predictive approach is based on the modified mechanics of cutting analysis, incorporating the "edge forces," and mathematically relates the developed cutting analyses of practical operations such as turning or milling to the fundamental or "classical" oblique cutting processes together with the values of basic cutting quantities found from "classical" orthogonal cutting tests (Armarego and Uthaichaya, 1977). The basic cutting quantities form a generic data bank for a particular tool-workpiece material combination and are used for all the practical machining operations which have been modelled. A feature of this approach is that the predictive models incorporate all the tool and cut geometrical variables and cutting conditions.

Contributed by the Manufacturing Engineering Division for publication in the JOURNAL OF MANUFACTURING SCIENCE AND ENGINEERING. Manuscript received July 1994; revised Dec. 1994. Associate Technical Editor: D. Stephenson.

Furthermore this approach is ideally suited for modular software development. A CAD system and data base has been developed in predicting turning, drilling, peripheral and face milling operations using the orthogonal cutting data base and oblique cutting analyses model (Armarego and Deshpande, 1993). Furthermore, the machining operations can be simulated and optimized by integrating the data base and process mechanics to NC tool path generation in CAD/CAM systems (Altintas and Spence, 1991, 1994).

A comparison of the ‘‘mechanistic’’ approach and ‘‘unified mechanics of cutting’’ approach as applied to milling operations will show that the essential difference lies in the way the elemental force components acting on the active tooth elements are established. These elemental forces, once found, are used to develop mathematical models for predicting the force components and torque in each and every active tooth element on the cutter at any orientation angle from which total instantaneous force components and torque can be found. The fluctuations in the instantaneous force components as well as the average values for one tooth cycle or cutter orientation can then be found by varying the cutter orientation angle over the required range. However, in the mechanistic approach the element force components are found from the milling force coefficients obtained from special milling tests for the given cutter geometry (Koenigsberger and Sabberwal, 1961; Kline et al., 1982). By contrast in the unified mechanics of cutting approach the elemental forces are found from modeling the tooth elements as oblique cutting analysis and the relevant tool-workpiece material combination. In the latter approach the elemental forces can be predicted for any cutter geometrical design and specification. This would eliminate the need for the special milling tests for each cutter geometry as well as enable the available sophisticated mechanistic models and software for predicting the force, power, component surface errors and vibration stability characteristics for rigid and flexible milling systems to be used in process planning and milling cutter design.

In this paper a method for predicting the milling force component coefficients in three cartesian directions from the unified mechanics of cutting approach will be developed and experimentally verified by comparing the predicted and measured milling force coefficients as well as the average and fluctuating force components from milling tests. For this purpose the end milling operation will be considered when machining titanium alloy  $Ti_6Al_4V$  so that an orthogonal cutting data base will need to be experimentally established.

Henceforth the paper is organized as follows: The modelling of the milling forces for the prediction of the milling force coefficients from the mechanistic and mechanics of cutting approaches are outlined in Section 2. The experimental results and model verification are given in Section 3 followed by the conclusions in Section 4.

## 2 Modeling of Milling Forces

The general geometry of the end milling operation and coordinate system of axes is shown in Fig. 1(a). The elemental

tangential,  $dF_t$ , radial,  $dF_r$ , and axial  $dF_a$  cutting forces acting on flute  $j$  of an ‘‘ideal’’ system (with a rigid cutter and zero eccentricity in the cutter axis of rotation) are shown in Fig. 1(b) and given by

$$\begin{aligned} dF_{t_j}(\theta, z) &= [K_{te} + K_{tc}t_j(\theta, z)]dz \\ dF_{r_j}(\theta, z) &= [K_{re} + K_{rc}t_j(\theta, z)]dz \\ dF_{a_j}(\theta, z) &= [K_{ae} + K_{ac}t_j(\theta, z)]dz \end{aligned} \quad (1)$$

where  $t_j(\theta, z) = s_t \sin \theta_j(z)$  is the uncut chip thickness and  $s_t$  is the feed rate per tooth,  $\theta$  is the immersion (or cutter orientation) angle measured clockwise from the positive  $y$  axis to a reference flute  $j = 0$ , which has immersion  $\theta$  at its tip  $z = 0$ . On flute  $j$ , a differential chip element at the axial location  $z$  has an immersion angle  $\theta_j(z) = \theta + j\theta_p - k_i z$ , where  $\theta_p = 2\pi/N$  is the flute angular pitch and  $N$  is the number of teeth on the cutter. At an axial depth  $z$ , the angular helix lag of the differential element on tooth  $j$  from the leading point on the tooth’s cutting edge ( $z = 0$ ) is  $k_i z$  where  $k_i = \tan i/R$ , while  $i$  and  $R$  are the helix angle and the cutter radius, respectively. The cutting forces in Eq. (1) are modelled in terms of two fundamental phenomena, an *edge force* component due to rubbing or ploughing at the cutting edge, represented by  $K_{te}$ ,  $K_{re}$  and  $K_{ae}$  on a unit width of cut basis, and a *cutting* component due to shearing at the shear zone and friction at the rake face, represented by  $K_{tc}$ ,  $K_{rc}$  and  $K_{ac}$  on a unit area of cut basis.

It should be noted that the above interpretation of the force functions in Eq. (1) is consistent with the notions of ‘‘edge’’ forces noted in the machining research literature (Thomsen et al., 1953; Kobayashi and Thomsen, 1959; Albrecht, 1960) and included in the modified mechanics of cutting analyses (Armarego, 1983; Armarego and Whitfield, 1985) used in the unified mechanics of cutting approach to milling considered later. Thus the elemental force components can be predicted if the various  $K$ ’s in Eq. (1) as well as the instantaneous cut proportions,  $t_j(\theta, z)$  and  $dz$  are known.

In a number of mechanistic models for the milling process the parameters  $K_{te}$ ,  $K_{re}$ ,  $K_{ae}$ ,  $K_{tc}$ ,  $K_{rc}$ ,  $K_{ac}$  are referred to as the *milling force coefficients* and are established from specially devised milling tests and mechanistic analysis. In the mechanics of cutting approach the parameters can be predicted from the oblique cutting analysis and the basic cutting quantities from the orthogonal cutting data base. These two methods will be outlined below.

**Mechanistic Evaluation of Milling Force Coefficients.** In order to evaluate the milling force coefficients a set of slot milling experiments at different feeds per tooth and cutting speeds using a constant cutting geometry have to be run. The evaluated coefficients are valid only for the specific cutter geometry tested, and a set of milling tests are required for each cutter geometry. The milling coefficients are evaluated from a

### Nomenclature

$a$ = axial depth of cut	$i$ = helix angle or angle of obliquity	$s_t$ = feed per tooth
$b$ = width of cut	$K_{tc}, K_{rc}, K_{ac}$ = tangential, radial and axial cutting force coefficients in milling	$t, t_c$ = cut and chip thickness in orthogonal cutting, respectively
$dF_t, dF_r, dF_a$ = differential tangential, radial and axial cutting forces in milling	$K_{te}, K_{re}, K_{ae}$ = tangential, radial and axial edge force coefficients in milling	$\alpha_r, \alpha_n$ = radial and normal rake angles
$F_P, F_Q$ = power and thrust force components in orthogonal cutting	$R$ = cutter radius	$\beta$ = friction angle at the rake face
$F_x, F_y, F_z$ = milling forces in feed, $x$ , normal, $y$ , and axial; $z$ , directions on flute $j$	$r_t, r_i$ = chip length and thickness ratios in orthogonal cutting, respectively	$\phi$ = shear angle in orthogonal cutting
		$\phi_n, \beta_n$ = normal shear and friction angles in oblique cutting, respectively
		$\eta_c$ = chip flow angle in the rake face
		$\tau$ = shear stress at the shear plane

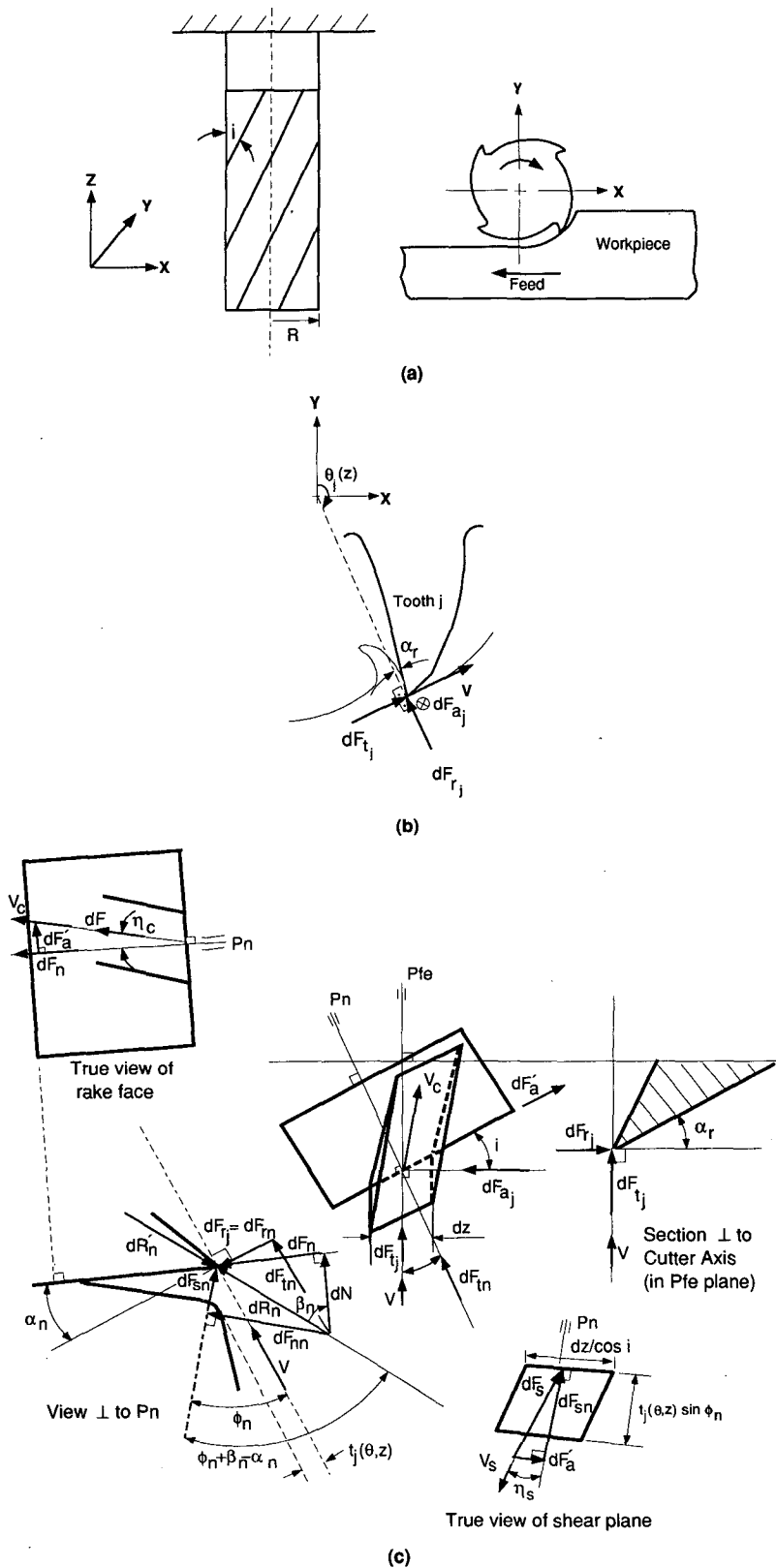


Fig. 1 (a) Geometry of milling process (b) components of milling forces (c) oblique cutting model for a milling tooth element

comparison of the linear equations relating the average force components per tooth period to the feed per tooth established from the slot milling experimental data and derived from the mechanistic analysis.

In developing the average force per tooth equations, the elemental forces are resolved into the feed ( $x$ ) and normal ( $y$ ) directions and integrated along the in cut portion of the flute  $j$  to obtain the total cutting force produced by the flute.

$$F_{x_j}(\theta) = \frac{R}{\tan i} \left[ K_{te} \sin \theta(z) - K_{re} \cos \theta(z) + \frac{S_t}{4} (K_{rc}(2\theta(z) - \sin 2\theta(z)) - K_{tc} \cos 2\theta(z)) \right]_{z_{j,1}(\theta)}^{z_{j,2}(\theta)}$$

$$F_{y_j}(\theta) = -\frac{R}{\tan i} \left[ -K_{re} \sin \theta(z) - K_{te} \cos \theta(z) + \frac{S_t}{4} (K_{tc}(2\theta(z) - \sin 2\theta(z)) + K_{rc} \cos 2\theta(z)) \right]_{z_{j,1}(\theta)}^{z_{j,2}(\theta)}$$

$$F_{z_j}(\theta) = \frac{R}{\tan i} [K_{ae}\theta(z) - s_t K_{ac} \cos \theta(z)]_{z_{j,1}(\theta)}^{z_{j,2}(\theta)} \quad (2)$$

where  $z_{j,1}(\theta)$  and  $z_{j,2}(\theta)$  are the lower and upper axial engagement limits of the in cut portion of the flute  $j$ . The cutting forces contributed by all flutes are calculated and summed to obtain the total instantaneous forces on the cutter at immersion  $\theta$ .

$$F_x(\theta) = \sum_{j=0}^{N-1} F_{x_j}; \quad F_y(\theta) = \sum_{j=0}^{N-1} F_{y_j}; \quad F_z(\theta) = \sum_{j=0}^{N-1} F_{z_j}; \quad (3)$$

The average milling forces per tooth period are  $\bar{F}_x$ ,  $\bar{F}_y$  and  $\bar{F}_z$ , and can be found by integrating Eq. (2) over one full rotation of the cutter,

$$\left. \begin{aligned} \bar{F}_x &= -K_{te}S + K_{re}T - \frac{S_t}{4} (-K_{tc}P + K_{rc}Q) \\ \bar{F}_y &= -K_{te}T - K_{re}S + \frac{S_t}{4} (K_{tc}Q + K_{rc}P) \\ \bar{F}_z &= -\frac{aN}{2\pi} K_{ae}(\theta_{ex} - \theta_{st}) + s_t K_{ac}T \end{aligned} \right\} \quad (4)$$

where

$$P = \frac{aN}{2\pi} [\cos 2\theta]_{\theta_{st}}^{\theta_{ex}}; \quad Q = \frac{aN}{2\pi} [2\theta - \sin 2\theta]_{\theta_{st}}^{\theta_{ex}}$$

$$S = \frac{aN}{2\pi} [\sin \theta]_{\theta_{st}}^{\theta_{ex}}; \quad T = \frac{aN}{2\pi} [\cos \theta]_{\theta_{st}}^{\theta_{ex}} \quad (5)$$

$\theta_{st}$  and  $\theta_{ex}$  are the start and exit angles of the cut and  $a$  is the axial depth of cut. A set of milling experiments are conducted at different feed rates but constant immersion and axial depth of cut. Since slot milling experiments are conducted, the entry and exit angles are  $\theta_{st} = 0$  and  $\theta_{ex} = \pi$ , respectively. The parameters  $P$ ,  $Q$ ,  $S$ ,  $T$  in Eq. (5) are constant for all experiments, therefore the average cutting forces can be expressed by a linear function of feed rate ( $s_t$ ) and an offset contributed by the edge force component.

$$\bar{F}_q = \bar{F}_{qe} + s_t \bar{F}_{qc} \quad (q = x, y, z) \quad (6)$$

The average forces at each feed rate are measured, and edge-cutting components ( $\bar{F}_{qe}$ ,  $\bar{F}_{qc}$ ) are estimated by a linear regression of the data. Finally, the cutting force coefficients are evaluated from Eqs. (4) and (6) as follows:

$$K_{te} = -\frac{\bar{F}_{xe}S + \bar{F}_{ye}T}{S^2 + T^2}; \quad K_{tc} = 4 \frac{\bar{F}_{xc}P + \bar{F}_{yc}Q}{P^2 + Q^2}$$

$$K_{re} = \frac{K_{te}S + \bar{F}_{xe}}{T}; \quad K_{rc} = \frac{K_{tc}P - 4\bar{F}_{xc}}{Q}$$

$$K_{ae} = -\frac{2\pi}{aN} \frac{\bar{F}_{ze}}{\theta_{ex} - \theta_{st}}; \quad K_{ac} = \frac{\bar{F}_{zc}}{T} \quad (7)$$

The procedure is repeated for each cutter geometry, hence

the milling force coefficients cannot be predicted prior to testing of newly designed cutters using mechanistic models. Furthermore, mechanistic models do not provide a physical insight to the influence of material properties, lubricant and cutter geometry on the cutting mechanics.

**Prediction of Milling Force Coefficients from an Oblique Cutting Model.** In order to predict the milling force coefficients it is first necessary to establish the relevant equations from the oblique cutting model. The cutting action of the helical teeth at the periphery of end milling cutter can be represented as "classical" oblique cutting processes with an angle of inclination (or obliquity) equal to the helix angle  $i$  and a normal rake angle  $\alpha_n$ , which is related to the specified radial rake angle  $\alpha_r$  and helix angle  $i$  (Armarego and Brown 1969)

$$\tan \alpha_n = \tan \alpha_r \cos i \quad (8)$$

The elemental deformation geometry, velocities and forces of the thin shear zone oblique cutting model at an active tooth element are shown in Fig. 1(c), where the relationship between the radial rake  $\alpha_r$ , the normal rake  $\alpha_n$  and the helix or inclination angle  $i$  are illustrated. In this model the elemental axial width  $dz$  is considered to be narrow enough to ignore any variations across the width, e.g.,  $t_f(\theta, z)$  variations. The similarity between this model and that of the "classical" oblique cutting process and the modified mechanics of cutting analyses documented in detail in textbooks (Armarego and Brown, 1969) and the literature (Armarego et al., 1977, 1985, 1990, 1993) is evident when allowances are made for the fact that the instantaneous radial cut thickness  $t_f(\theta, z)$  and elemental axial width  $dz$  correspond to the cut thickness  $t$  and width of cut  $b$  in "classical" oblique cutting and the element tangential, radial and axial force components  $dF_{tj}$ ,  $dF_{rj}$  and  $dF_{aj}$  correspond to the power, thrust and radial components  $F_P$ ,  $F_Q$  and  $F_R$  in the "classical" process. Thus the elemental friction force  $dF$  and chip velocity  $V_c$  in the rake face are collinear and inclined at the acute angle  $\eta_c$  to the normal plane  $P_n$  while the elemental shear force  $dF_s$  and shear velocity  $V_s$  in the "shear plane" are collinear and included at the acute angle  $\eta_s$  to  $P_n$ , i.e., collinearity conditions apply as shown in Fig. 1(c). Furthermore, the chip is considered to be in equilibrium under the action of two equal, opposite and collinear forces acting on the chip at the "shear plane" and tool-chip interface while the continuity and incompressibility conditions apply. Based on the modified mechanics of cutting analysis (Armarego et al., 1977, 1985, 1990, 1993) the three elemental forces  $dF_{tj}$ ,  $dF_{rj}$  and  $dF_{aj}$  in Fig. 1(c) consist of a "cutting" component found from the analysis of Fig. 1(c) and an "edge force" component due to rubbing or ploughing at the cutting edge. Thus the element force components functions in Eq. (1) are compatible with those of the above cutting analysis.

From force equilibrium of the chip in Fig. 1(c) the milling force coefficients due to "cutting" in Eq. (1), i.e.,  $K_{tc}$ ,  $K_{rc}$  and  $K_{ac}$ , can be expressed in terms of the modified mechanics of cutting analysis variables as follows (Armarego and Brown, 1969; Armarego, 1985)

$$K_{tc} = \frac{\tau}{\sin \phi_n} \frac{\cos(\beta_n - \alpha_n) + \tan \eta_c \sin \beta_n \tan i}{c}$$

$$K_{rc} = \frac{\tau}{\sin \phi_n \cos i} \frac{\sin(\beta_n - \alpha_n)}{c}$$

$$K_{ac} = \frac{\tau}{\sin \phi_n} \frac{\cos(\beta_n - \alpha_n) \tan i - \tan \eta_c \sin \beta_n}{c} \quad (9)$$

where

$$c = \sqrt{\cos^2(\phi_n + \beta_n - \alpha_n) + \tan^2 \eta_c \sin^2 \beta_n}$$

while the normal friction angle  $\beta_n$ , i.e., the component of the

friction angle  $\beta$  ( $=\tan^{-1}(dF/dN)$ ) in the normal plane  $P_n$ , is given by

$$\tan \beta_n = \tan \beta \cos \eta_c \quad (10)$$

and from the deformation geometry in Fig. 1(c) and continuity and incompressibility conditions, the normal shear angle  $\phi_n$  in the normal plane  $P_n$  is given by

$$\tan \phi_n = \frac{r_t \cos \alpha_n}{1 - r_t \sin \alpha_n} = \frac{r_l(\cos \eta_c / \cos i) \cos \alpha_n}{1 - r_l(\cos \eta_c / \cos i) \sin \alpha_n} \quad (11)$$

where  $r_t$  and  $r_l$  are chip thickness and chip length ratios. Furthermore, allowing for collinearity between the friction force and chip velocity direction in the rake face as well as between the shear force and shear velocity directions in the primary shear zone (or plane) as shown in Fig. 1(c), the following well known equation (Armarego et al., 1969, 1983, 1985; Whitfield, 1986) applies to "classical" oblique cutting processes

$$\tan(\phi_n + \beta_n) = \frac{\cos \alpha_n \tan i}{\tan \eta_c - \sin \alpha_n \tan i} \quad (12)$$

Combining Eqs. (9)–(12), the milling force coefficients given in Eq. (9) can be expressed in the following alternative general functional forms,

$$\begin{aligned} K_{tc}, K_{rc}, K_{ac} &= \text{functions}(\tau, \alpha_n, i, \phi_n \text{ or } r_l, \beta_n \text{ or } \beta) \quad \text{or,} \\ K_{tc}, K_{rc}, K_{ac} &= \text{functions}(\tau, \alpha_n, i, \phi_n \text{ or } r_l, \eta_c) \quad \text{or,} \\ K_{tc}, K_{rc}, K_{ac} &= \text{functions}(\tau, \alpha_n, i, \eta_c, \beta_n \text{ or } \beta) \quad (13) \end{aligned}$$

Thus these coefficients can be evaluated if the elemental tool geometry  $\alpha_n$ ,  $i$ , the work material shear stress  $\tau$  and any two of the three basic cutting quantities  $\phi_n$  or  $r_l$ ,  $\beta_n$  or  $\beta$  and  $\eta_c$  are known.

The common method of solutions of Eqs. (9)–(12) to predict the three coefficients in Eq. (9) is to use the values of three basic cutting quantities, namely; the shear stress  $\tau$ , the chip length ratio  $r_l$  and the friction angle  $\beta$  at the rake face, from the appropriate data bank found from "classical" orthogonal cutting tests, i.e., adopt the first alternative in Eq. (13). This method involves a numerical solution of Eqs. (10), (11) and (12) to predict the chip flow angle  $\eta_c$  given  $r_l$  and  $\beta$  from which  $\eta_c$ , together with the corresponding normal shear angle  $\phi_n$  and normal friction angle  $\beta_n$  from Eqs. (10) and (11) as well as the shear stress  $\tau$  from the data bank for the known elemental geometry  $\alpha_n$  and  $i$  can be substituted in Eq. (9) to determine the three coefficients. The evidence and rationale for this method of solution has been well documented in the literature.

Similarly the milling force component coefficient due to the edge forces, i.e.,  $K_{te}$ ,  $K_{re}$  and  $K_{ae}$  can be found from the orthogonal cutting data base values for the appropriate tool-workpiece combination and cutting conditions. These coefficients are represented by the intercept force components per unit cut width of the force-cut thickness functions at zero cut thickness. As such the  $K_{ae}$  value, which is known to be very small in oblique cutting, is usually taken as zero (Armarego and Whitfield, 1985), although alternative estimates have sometimes been used (e.g.,  $K_{ae} = K_{tc} \sin i$ ) (Armarego and Deshpande, 1993).

In this approach an orthogonal data base has to be established for the given tool-workpiece material combination as noted earlier. This involves running a comprehensive set of orthogonal cutting tests at various cut thickness  $t$  values, rake angles  $\alpha_n$  and cutting speeds  $V$  and measuring the two force components along the cutting speed direction  $F_p$  and normal to  $V$  and the machined surface,  $F_Q$  as well as the chip length ratio  $r_l$  or chip thickness ratio  $r_t$  (since  $r_t = r_l$ ). These two force components correspond to the elemental tangential and radial force component directions in Eq. (1) for milling. The edge force components are estimated from the intercepts of the measured force-cut thickness functions at zero cut thickness and are subtracted

**Table 1 Cutting force coefficients for different rake angles as transformed from the orthogonal data and identified from milling tests. Material: Ti<sub>6</sub>Al<sub>4</sub>V; units ( $K_{te}$ ,  $K_{rc}$ ,  $K_{ac}$ ) = [N/mm<sup>2</sup>], ( $K_{te}$ ,  $K_{re}$ ,  $K_{ae}$ ) = [N/mm].**

$\alpha_n$ (deg)	Milling Test						Predicted		
	$K_{te}$	$K_{tc}$	$K_{re}$	$K_{rc}$	$K_{ae}$	$K_{ac}$	$K_{tc}$	$K_{rc}$	$K_{ac}$
0	29.7	1825	55.7	770	1.8	735	1963	646	778
5	24.7	1698	42.9	438	5.5	591	1805	461	699
12	22.7	1731	44.5	317	2.4	623	1619	253	604

from the measured forces  $F_p$  and  $F_Q$  to estimate the forces due to cutting  $F_{pc}$  and  $F_{qc}$ , respectively. The shear angle  $\phi$ , shear stress  $\tau$  in the shear zone and the friction at the rake face  $\beta$  are calculated from the measured cutting forces and chip length or thickness ratios using the well known orthogonal cutting model equations (Merchant, 1944)

$$\left. \begin{aligned} \tan \phi &= \frac{r_l \cos \alpha}{1 - r_l \sin \alpha} = \frac{r_l \cos \alpha}{1 - r_l \sin \alpha} \\ \tau &= \frac{(F_{pc} \cos \phi - F_{qc} \sin \phi) \sin \phi}{bt} \\ \tan \beta &= \frac{F_{qc} + F_{pc} \tan \alpha}{F_{pc} - F_{qc} \tan \alpha} \end{aligned} \right\} \quad (14)$$

The edge force components and basic cutting quantities have to be statistically processed to study the effects of the process variables as well as to establish "best fit" equations for inclusion in the data base (Armarego et al., 1983, 1985).

### 3 Experimental Results and Model Verification

Several orthogonal cutting and milling tests have been performed on a titanium alloy (Ti<sub>6</sub>Al<sub>4</sub>V) for the verification of the method. The milling force coefficient are evaluated both from the milling tests using mechanistic approach and from orthogonal cutting tests using oblique cutting model. They are compared in predicting the milling forces.

**Mechanistic Model Results.** A set of full immersion milling tests were conducted with carbide end mills with single flute, 30 deg helix angle and 19.05 mm diameter. The axial depth of cut and the cutting speed were constant at 5.08 mm and 30 m/min, respectively. The maximum chip thickness (feed-per-tooth) range of 0.0127–0.1 mm was considered. Helical end mills with normal rake angles of 0 deg, 5 deg, 12 deg were used to determine the robustness of the method for different geometries. The cutting forces in three directions were measured using a Kistler table dynamometer, and average values were found at each feed rate. The edge and milling force coefficients were predicted from the average forces using mechanistic Eq. (7). Since the mechanistically evaluated coefficients are valid only for a fixed cutter geometry, the procedure had to be repeated for all three cutters. The mechanistically determined cutting coefficients from milling tests are shown in Table 1. It can be noticed that the edge force coefficients in the axial direction ( $K_{ae}$ ) are negligibly small.

**Oblique Model Results.** A set of turning tests with tools having zero inclination angle were performed on titanium tubes in order to achieve ideal orthogonal cutting conditions. The outer diameter and the wall thickness of the tubes used were 100 mm and 3.8 mm, respectively. The cutting speed range of 3–47 m/min and carbide tools with rake angles of (0 deg, 2 deg, 5 deg, 8 deg, 10 deg, 15 deg) were used, which covers the rake angle range of the end mills tested. The feed rate range of 0.005–0.1 mm was covered with 5 steps (0.005, 0.01, 0.03,

Table 2 Orthogonal cutting data (units:  $\alpha$  (deg),  $t$  [mm])

$\tau$	= 613 MPa
$\beta$	= $19.1 + 0.29\alpha$
$r_t$	= $r_o t^a$
$r_o$	= $1.755 - 0.028\alpha$
$a$	= $0.331 - 0.0082\alpha$
$K_{te}$	= 24 N/mm
$K_{re}$	= 43 N/mm

0.07, 0.1 mm). Very low cutting speeds were considered in order to see the effect of cutting speed, and also to be able to use the same data base for different milling cutter geometries such as ball end mills where the cutting speeds are close to zero at the ball end. For each case, chip thickness, tangential ( $F_p$ ) and feed ( $F_Q$ ) cutting force measurements were recorded. The chip thicknesses were measured with a micrometer, and an average thickness of five collected chips was considered. A more accurate method of chip thickness identification could have been the use of chip lengths and weights. However, this procedure was difficult in turning Titanium chips, which were very thin and curly. The cutting forces were measured by a Kistler dynamometer mounted on the tool post. All cutting tools had insignificant wear during the tests.

The edge forces are identified by extrapolating the cutting forces to zero cut thickness and, they are very close to each other for different cutting velocities and rake angles. Therefore, average values of the edge forces are used in the rest of the analysis. The mean and the standard deviation of the edge forces were  $K_{te} = 24$  N/mm with  $\sigma(K_{te}) = 6.3$  and  $K_{re} = 43$  N/mm with  $\sigma(K_{re}) = 7.3$ , respectively. The agreement between the edge force coefficients identified from milling tests and the orthogonal cutting suggests that the edge forces do not vary with the angle of obliquity (see Tables 1 and 2 for comparison). Also, the edge force in the axial direction is very small and therefore, it is neglected in the transformation of the orthogonal cutting data to oblique model. Figure 2 shows the variation of  $r_t$  with uncut chip thickness and rake angle. No significant variation was observed with the cutting velocity. As it can be seen from the figure,  $r_t$  exponentially varies with the cut thickness and the following empirical relationship was predicted by curve-fitting the expressions to orthogonal cutting data.

$$r_t = r_o t^a \quad a = 0.331 - 0.0082\alpha \quad r_o = 1.755 - 0.028\alpha. \quad (15)$$

Equation (15) implies that the cutting ratio  $r_t$  strongly varies

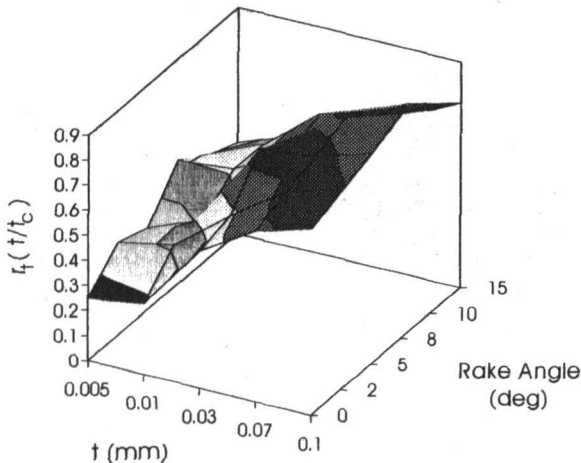


Fig. 2 Variation of cutting ratio in orthogonal tests

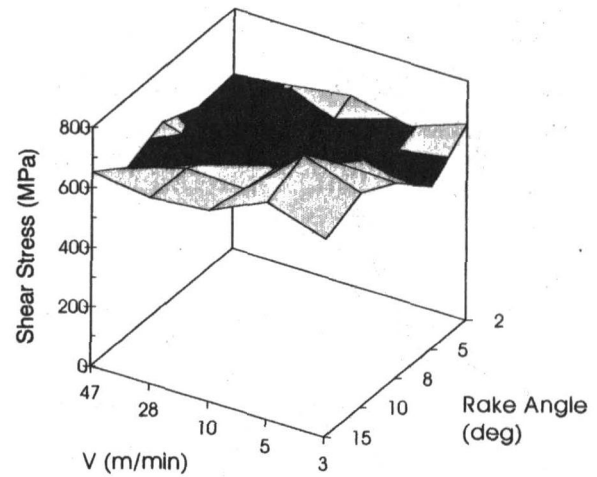


Fig. 3 Variation of the identified shear stress in orthogonal tests

with the uncut chip thickness, whereas the variation with the rake angle is quite small. The drop in cutting ratio at small chip thickness has been noted in some previous works, and can be attributed to the reduced effective rake angle at small chip thicknesses due to nose radius, rubbing and size effect phenomenon of metals. Cutting ratio obtained with high rake angles were compared, and the above relationship was found to be valid for the tools with a rake angle range of 0–35 deg.

The shear stress ( $\tau$ ) and friction angle ( $\beta$ ) are calculated from Eq. (14) and shown in Figs. 3 and 4. As it can be seen from Fig. 3, the shear stress does not vary significantly with velocity and rake angle. This is due to the opposite effects of the generated heat and the strain rate at the shear zone which are proportional to the cutting velocity. Therefore, an average value can be used for the shear stress. The average value and standard deviation of the shear stress were calculated as  $r = 613$  MPa with  $\sigma(\tau) = 73$ . The friction angle, on the other hand, slightly varies with the rake angle and the cutting velocity. The friction angle identified from the orthogonal cutting tests is the average value of the friction in the sticking and the sliding regions between the chip and the rake face of the tool. The friction coefficient is higher in the sliding region which becomes longer as the rake angle is increased due to the reduced pressure on the rake face. Hence, the average value of the friction on the rake face increases with the rake angle. The friction angle slightly varies with the cutting velocity as well, but this variation is mainly in the low cutting velocity range ( $V < 10$  m/min)

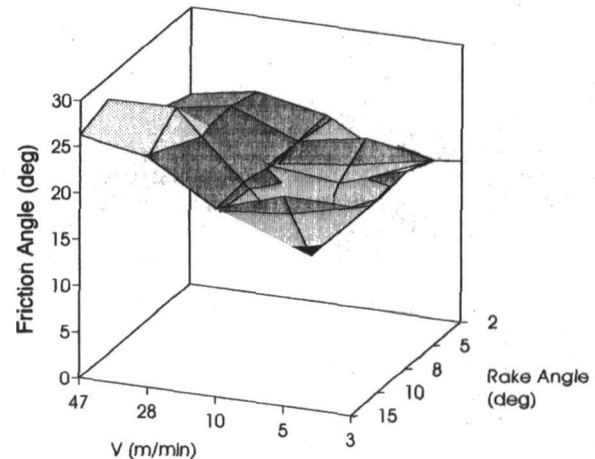


Fig. 4 Variation of the identified friction angle in orthogonal tests

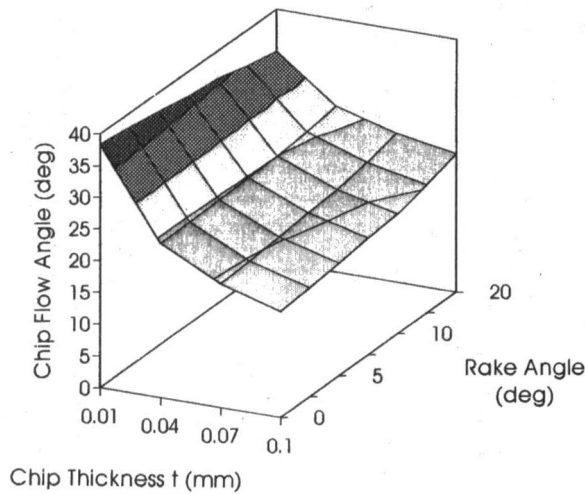


Fig. 5 Predicted values of chip flow angle by using orthogonal data for 30 deg helix angle

and it is almost constant in the practical cutting velocity range. Therefore, the variation of the friction coefficient with the cutting velocity is more important in the analysis of ball-end milling as the cutting velocity approaches to zero at the center of the ball (Yucesan and Altintas, 1996). Hence, the variation of the friction angle with the cutting velocity is neglected and the following equation for the friction angle  $\beta$  is obtained by linear regression of the data:

$$\beta = 19.1 + 0.29\alpha \quad (16)$$

where the rake angle  $\alpha$  and the friction angle  $\beta$  are in degrees. The mean value of the friction angle  $\beta$  is  $\bar{\beta} = 21.3$  deg with standard deviation of  $\sigma(\bar{\beta}) = 3.1$  for all rake angles tested here. Note that  $\beta$  is an average friction angle on the total chip-rake face contact zone which consists of sticking and sliding regions.

The mean values of the percentage error between the identified and the calculated values from the curve-fit equations are determined as:

$$\begin{aligned} \tau: & (-0.07 \text{ percent}), \quad \beta: (1.6 \text{ percent}), \quad (\bar{\beta}): (-2.3 \text{ percent}), \\ r: & (3.8 \text{ percent}), \quad K_{rc}: (-10.9 \text{ percent}), \quad K_{re}: (-5.1 \text{ percent}) \end{aligned}$$

The chip flow angle ( $\eta_c$ ) for 30 deg helix angle is computed from numerical solution of Eqs. (10)–(12) by using the orthogonal data, i.e.,  $r$ , and  $\beta$  for different rake angles. Figure 5 shows that  $\eta_c$  increases with normal rake angle ( $\alpha_n$ ) and decreases with the chip thickness and thus with cutting ratio  $r_t$  as well (see Fig. 2). The orthogonal cutting parameters are summarized in Table 2.

Using the transformation Eqs. (9) the cutting constants,  $K_{rc}$ ,  $K_{re}$  and  $K_{ac}$ , for the specific three test end mills, are calculated from the orthogonal cutting parameters ( $\tau$ ,  $\beta$ ,  $r$ ) and the chip flow angle ( $\eta_c$ ) (see Table 1). The same edge force coefficients,  $K_{re}$  and  $K_{rc}$ , that were identified from the orthogonal data were used for all end mills. An average chip thickness is calculated over a revolution of engagement. However, the accuracy can be improved if the average chip thickness is calculated over the engaged length of the helical flute, but at the expense of computing the coefficients at each rotational position of the cutter. The predicted milling force coefficients slightly vary with the average chip thickness as the cutting ratio and the chip flow angle are functions of the chip thickness, average values are given in Table 1. As it can be seen from Table 1, the milling force coefficients predicted from orthogonal cutting and mechanistically identified from milling tests are satisfactorily close to each other. While the orthogonal cutting data can be used to predict any helical end mill geometry, the mechanistically iden-

tified coefficients are unique for the specific end mill geometry which was used in calibration milling tests.

**Accuracy of Milling Force Prediction.** The accuracy of the milling force predictions using the milling force coefficient analysis evaluated from the orthogonal cutting data has been tested for over 20 milling experiments. The experiments were performed by using cutters with different rake angles (0, 5, 12, 15, 20) and number of teeth (1 and 4), axial depth of cut (5 and 7.5 mm), feed per tooth (0.0127, 0.025, 0.05, 0.1, 0.2 mm/tooth) and radial depth of cut (slotting, up and down milling-half immersion). The percentage deviations of the average and the maximum cutting force predictions from the measurements are shown in Fig. 6. About 80 percent of the force predictions in  $x$  and  $y$  directions have less than  $\pm 10$  percent deviation and the maximum deviation in all cases is less than 25 percent. The predictions for the  $z$  direction, however, have less accuracy as it can be seen from the figure. This can be attributed to the fact that no edge force has been used for the  $z$  direction. Although, the edge force in  $z$  direction is very small compared to  $x$  and  $y$  directions as shown in Table 1, at small chip thickness its contribution may become significant. Also, the noise in force measurements may affect the results as the cutting forces in  $z$  direction are relatively small ( $<100$  N for most of the cases considered in the statistical analysis).

One half immersion up milling and one half immersion down milling tests are used to examine the accuracy of the instantaneous force predictions. Figure 7 shows the measured and the predicted milling forces for a half immersion-up milling cutting test using a 19.05 mm diameter, four flute end mill. The feed per tooth is  $s_t = 0.05$  mm/tooth and the normal rake angle is 12 deg. The axial depth of cut and the cutting speed were 5.08 mm and 30 m/min, respectively. The force predictions based on the coefficients identified mechanistically from the slot millings tests and those transferred from the orthogonal data by calculating  $\eta_c$  show good agreement with the measured values. Figure 8 shows the predicted and measured forces for a half immersion-down milling test with four flute end mill where feed-rate  $s_t = 0.0127$  mm/tooth and the rake angle is 0 deg; the other conditions were the same as in up milling. Because the chip thicknesses removed in production of jet engine components made of  $Ti_6Al_4V$  alloy are rather small ( $<0.050$  mm), the maximum radial run outs are required to be less than 0.005 mm in order to avoid uneven loading of the flutes. This is accomplished by grinding the cutters on 8 axis precision CNC cutter grinders, and using recently available hydraulic chucks which apply uniform pressure to clamp cylindrical collets on the cutter shank. This technique produced radial run out of less than 0.005 mm on the ends of the four fluted cutters used in the experiments. The absence of unevenness among four periodic force wave forms shown in Figs. 7 and 8 indicate the effectiveness of the technique in minimizing the run-out on the cutters even when the feed rate is very low (0.0127 mm/flute in Fig. 8). However, the influence of run-out geometry and spindle tilt can be integrated to the cut thickness calculation as presented by Kline and DeVor (1983), and Armarego and Deshpande (1993).

The accuracy of the force predictions by using transformed data is almost the same as the accuracy obtained by the milling test calibrated coefficients. Note that the mechanistic model is basically curve fitting constants to milling test data, thus even it may seem to be slightly more accurate it is not practical in cutter design and process planning. However, as illustrated here, the orthogonal data can be used for milling force predictions and tool design with a satisfactory accuracy. Cutting forces produced by other oblique cutting operations, such as drilling and turning, can also be predicted using the same orthogonal cutting data and geometric transformation. The generalized method is therefore quite useful in developing a machining data base for process planners and tool designers.

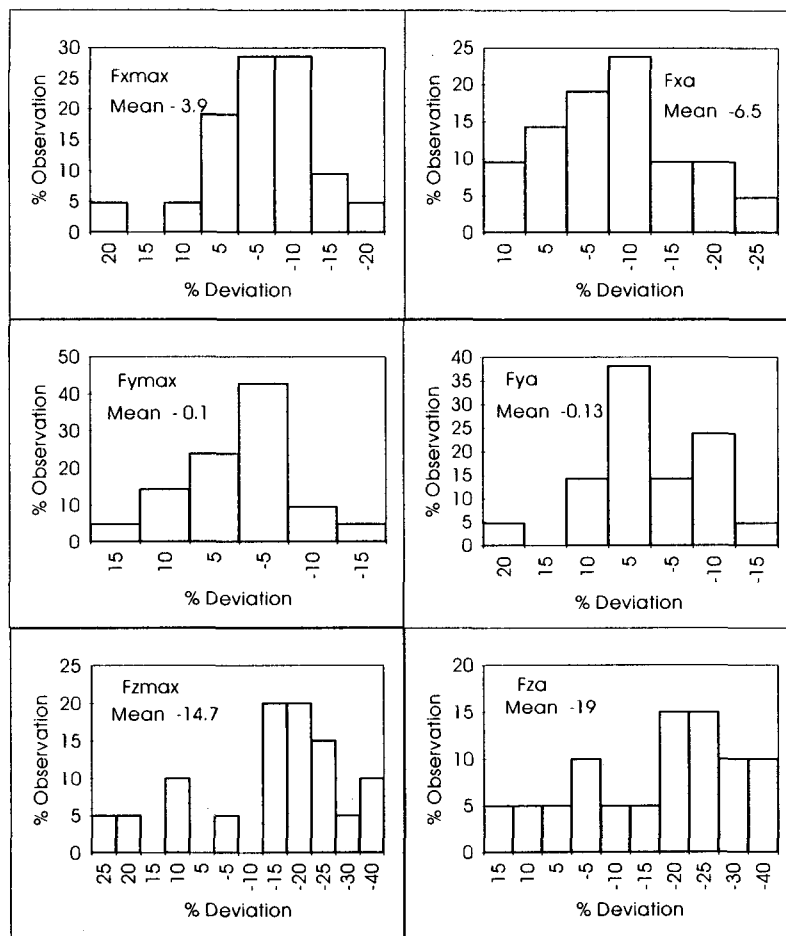


**Fig. 6** The statistical error analysis of the milling force predictions. The percentage error between the milling force predictions and the measured values were determined for 20 different milling tests.

#### 4 Conclusions

From a comparison of the mechanistic and unified mechanics of cutting approaches to milling force predictions, a method has been developed to predict the milling force coefficients for use in the former approach. The method involves the establishment of a data base of basic cutting quantities such as the shear stress, shear angle and friction angle at the rake face from a set of orthogonal cutting tests at various cutting conditions and rake angles together with the modified thin shear zone (or plane) analysis of classical oblique cutting incorporating the "edge"

forces. The method was specifically illustrated to predict the milling force coefficients and cutting forces in end milling of Titanium alloy ( $Ti_6Al_4V$ ). It is shown that the proposed method closely agrees with mechanistically calibrated cutting force coefficients. The mechanistic method requires a set of cutting tests for each milling cutter geometry whereas the proposed method require a set of standard orthogonal cutting tests which can be extended to any cutter geometry without milling cutter calibration tests. The approach allows designing a common orthogonal cutting data base, which can be used to predict cutting forces

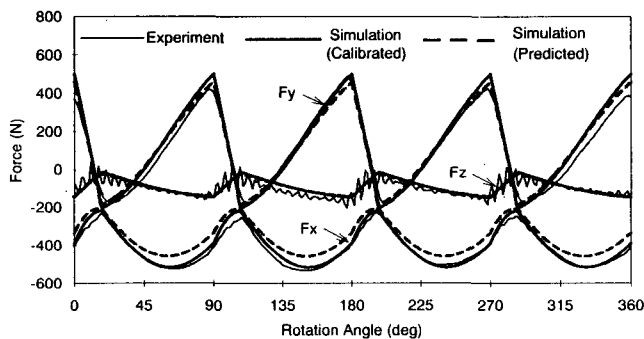


**Fig. 7** Milling forces measured and predicted by using milling test identified and transformed cutting force coefficients (half immersion-dry up milling,  $s_t = 0.05$  mm/tooth,  $a = 5.08$  mm,  $\alpha = 12$  deg, cutter diameter = 19.05 mm, cutting speed = 30 m/min)

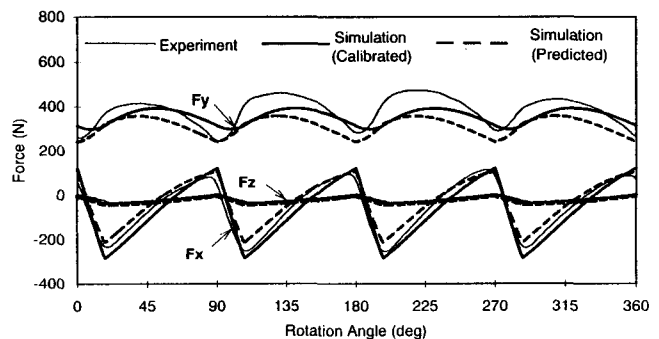


**Fig. 8** Milling forces measured and predicted by using milling test identified and transformed cutting force coefficients (half immersion-dry down milling,  $s_t = 0.0127$  mm/tooth,  $a = 5.08$  mm,  $\alpha = 0$  deg, cutter diameter = 19.05 mm, cutting speed = 30 m/min)

in variety of oblique machining operations. Integration of such a data base to NC tool path generation algorithms in CAD/CAM systems allows process planners to generate optimal, chatter and tool breakage free tool paths. The data base is also useful in analyzing the performance of different cutter design geometries prior to cutting tests.

## Acknowledgment

This research is supported by Natural Sciences and Engineering Research Council of Canada and Pratt & Whitney Aircraft of Canada.

## References

- Albrecht, P., 1960, "New Developments in the Theory of the Metal Cutting Process, Part I: The Ploughing Process in Metal Cutting," *ASME JOURNAL OF ENGINEERING FOR INDUSTRY*, Vol. 82, pp. 348–358.
- Altintas, Y., and Budak, E., 1992, "Peripheral Milling of Flexible Structures," *Materials Issues in Machining and the Physics of Machining Processes*, pp. 97–109, ASME Winter Annual Meeting, Anaheim, CA.
- Altintas, Y., and Spence, A., 1991, "End Milling Force Algorithms for CAD Systems," *Annals of the CIRP*, Vol. 40, No. 1, pp. 31–34.
- Armarego, E. J. A., 1983, "Practical Implications of Classical Thin Shear Zone Cutting Analyses," *UNESCO/CIRP Seminar on Manufacturing Technology*, pp. 167–182, Singapore.
- Armarego, E. J. A., and Brown, R. H., 1969, *The Machining of Metals*, Prentice-Hall.
- Armarego, E. J. A., and Deshpande, N. P., 1993, "Force Prediction Models and CAD/CAM Software for Helical Tooth Milling Processes, Part I, Basic Approach and Cutting Analyses," Vol. 31, No. 8, pp. 1991–2009, "Part II, Peripheral Milling Operations," Vol. 31, No. 10, pp. 2319–2336, "Part III, End-milling and Slotting Operations," *in press, International Journal of Production Research*.
- Armarego, E. J. A., Smith, A. J. R., and Gong, Z. J., 1990, "Four Plane Facet Point Drills-Basic Design and Cutting Model Predictions," *Annals of the CIRP*, Vol. 39, No. 1, pp. 41–45.
- Armarego, E. J. A., and Uthachaya, M., 1977, "A Mechanics of Cutting Approach for Force Prediction in Turning Operations," *Journal of Engineering Production*, Vol. 1, No. 1, pp. 1–18.
- Armarego, E. J. A., and Whitfield, R. C., 1985, "Computer Based Modelling of Popular Machining Operations for Force and Power Predictions," *Annals of the CIRP*, Vol. 34, pp. 65–69.
- Boston, O. W., Gilbert, W. W., and Kaiser, K. B., 1937, "Power and Forces in Milling SAD 3150 with Helical Mills," *Transactions of the ASME*, Vol. 59, No. 2, pp. 545.
- Budak, E., and Altintas, Y., 1992, "Flexible Milling Force Model For Improved Surface Error Predictions," *Proceedings of the 1992 Engineering System Design and Analysis, Istanbul, Turkey*, pp. 89–94, ASME, PD-Vol. 47-1.
- Kline, W. A., DeVor, R. E., and Shareef, I. A., 1982, "The Prediction of Surface Accuracy in End Milling," *ASME JOURNAL OF ENGINEERING FOR INDUSTRY*, Vol. 104, pp. 272–278.
- Kline, W. A., DeVor, R. E., and Shareef, I. A., 1983, "The Effect of Runout on Cutting Geometry and Forces in End Milling," *International Journal of Machine Tool Design and Research*, Vol. 23, pp. 123–140.
- Kobayashi, S., and Thomsen, E. G., 1959, "Some Observations of the Shearing Process in Metal Cutting," *ASME JOURNAL OF ENGINEERING FOR INDUSTRY*, Vol. 81, pp. 251–262.
- Koenigsberger, F., and Sabberwal, A. J. P., 1961, "An Investigation into the Cutting Force Pulsations During Milling Operations," *International Journal of Machine Tool Design and Research*, Vol. 1, pp. 15–33.
- Martellotti, M. E., 1941, "An Analysis of the Milling Process," *Transactions of the ASME*, Vol. 63, pp. 677–700.
- Merchant, M. E., 1944, "Basic Mechanics of the Metal Cutting Process," *ASME Journal of Applied Mechanics*, pp. A-168–175.
- Montgomery, D., and Altintas, Y., 1991, "Mechanism of Cutting Force and Surface Generation in Dynamic Milling," *ASME JOURNAL OF ENGINEERING FOR INDUSTRY*, Vol. 113, pp. 160–168.
- Smith, S., and Tlustý, J., 1991, "An Overview of Modelling and Simulation of the Milling Process," *ASME JOURNAL OF ENGINEERING FOR INDUSTRY*, Vol. 113, No. 2, pp. 169–175.
- Spence, A., and Altintas, Y., 1994, "A Solid Modeller Based Milling Process Simulation and Planning System," *ASME JOURNAL OF ENGINEERING FOR INDUSTRY*, Vol. 116, No. 1, pp. 61–69.
- Sutherland, J. W., and DeVor, R. E., 1986, "An Improved Method for Cutting Force and Surface Error Prediction in Flexible End Milling Systems," *ASME JOURNAL OF ENGINEERING FOR INDUSTRY*, Vol. 108, pp. 269–279.
- Thomsen, E. G., Lapsley, J. R., and Grassi, R. C., 1953, "Deformation Work Absorbed by the Workpiece During Metal Cutting," *Transactions of the ASME*, Vol. 45, pp. 591–603.
- Tlustý, J., and MacNeil, P., 1975, "Dynamics of Cutting Forces in End Milling," *Annals of the CIRP*, Vol. 24, pp. 21–25.
- Whitfield, R. C., 1986, "A Mechanics of Cutting Approach for the Prediction of Forces and Power in Some Commercial Machining Operations," Ph.D. thesis, University of Melbourne.
- Yellowley, I., 1985, "Observations of the Mean Values of Forces, Torque and Specific Power in the Peripheral Milling Process," *International Journal of Machine Tool Design and Research*, Vol. 25, No. 4, pp. 337–346.
- Yucesan, G., and Altintas, Y., 1996, "Prediction of Ball End Milling Forces," *ASME JOURNAL OF ENGINEERING FOR INDUSTRY*, Vol. 118, No. 1, Feb., pp. 95–103.